NRL Report 6266

Scaling Underwater Exploding Wires

J. R. McGRATH

Energy Conversion Branch
Electronics Division

December 17, 1965

U.S. NAVAL RESEARCH LABORATORY
Washington, D.C.

CONTENTS

Scaling Underwater Exploding Wires

J. R. McGrath

Energy Conversion Branch
Electronics Division

Five-mil Nichrome wires have been exploded under water using a 1/2-μf capacitor which stored energy up to 100 joules. The results indicate that peak pressure scales like a chemical explosive if losses due to the circuit and joule heating of the wire itself are accounted for. On this basis, the equivalent weight of TNT represented by the electrical energy stored in the capacitor is

$$W = 525(0.325CV_0^2 - E_V)/H_D$$

where W is the weight in micropounds, C is the capacitance in farads, V_0 is the initial charging voltage, E_V is the estimated energy dissipated by the wire in joules, and H_D is the heat of detonation of TNT in calories per gram. This scaling behavior extends the law of similarity six decades in terms of weight, from pounds to micropounds. The peak pressure for exploding-wire phenomena has been obtained from data and is empirically expressed as

$$p_m = 26{,}800\,(W^{1/3}/R)^{1.08}$$

where p_m is peak pressure and R is pressure-gage distance.

The instrument response to the short-duration shock wave gives rise to a new definition of the explosion constant τ_e. The reduced time-constant parameter shows qualitative agreement in value and slope with chemical data scales, and is given empirically as:

$$\frac{\tau_e}{W^{1/3}} = 70\left(\frac{W^{1/3}}{R}\right)^{-0.22}$$

INTRODUCTION

This study relates the research areas of exploding-wire phenomena (EWP) and chemical underwater explosions (CUE). In this report the relevant theories and experiments of each field are outlined; and upon this relationship the purpose of this study is established.

Exploding-Wire Phenomena

Since Nairne (1) first reported his EWP experiments in 1774, considerable research has been conducted on this subject. At the present time, most of the phenomenological aspects have been explored in some depth. In the last two decades, considerable information has been amassed with the aid of improved instrumentation, most notably the streak and framing camera, the Park current shunt, and the Mach-Zehnder interferometer. However, no universally accepted theory, explaining satisfactorily the complex events associated with exploding wires, has been established.

In the absence of a theory for EWP, the discussion of experimental work must, in justice, include a complete list of investigations, which exceeds the scope of this introduction. However, a comprehensive annotated bibliography of EWP experiments, equipment, first-order theories, and techniques is given by Chace and Watson (2). A historical review of EWP research trends has been compiled by McGrath (3). A monograph on exploding wires, drawn from the papers presented at three conferences devoted to the subject, has been edited by Chace and Moore (4). General discussions of the processes taking place in an exploding wire by Bennett (5) and

NRL Problem E01-01; ONR Problem RR 010-04-41-5950; BuShips Problem SR 007-12-01-0800. This is an interim report on one phase of the problem; work on this and other phases is continuing. Manuscript submitted April 4, 1965.

Chace (6) give some idea of the complexity of the phenomena and the increasingly sophisticated techniques used to observe it.

Review of Underwater Explosion Theory

In this section the concepts, theories, and experiments of chemical underwater explosions (CUE) which bear directly upon this study are outlined.

For comparison of one CUE event with another, resort is made in common practice to similarity curves. These curves, in turn, are based upon the principle of similarity which was first credited to Hilliar (7). A more comprehensive discussion of similarity and scaling is given by Snay (8). Essentially, this principle states

$$p_m(R,t) = p_m(nR, nt) \tag{1}$$

where p_m is the peak pressure, R is the pressure-gage distance, t is the time, and n is a constant. Physically, this means that if an explosive charge in the form of a cube having a side of length L is enlarged to a side of length nL, then the same pressure will be measured a distance nR away. The duration of the explosion wave increases by the factor n. The utility of this principle is that it facilitates the calculation of shock-wave parameters (peak pressure and time) for charges of different weights (equivalently, different volumes). Theoretically, the principle of similarity satisfies the basic equations of motion of a fluid and, for a shock wave, the Rankine-Hugoniot relations. Experimentally the principle of similarity is important because pressure and time functions can be determined by measurements by varying either R or the charge size (volume). The other variable is determined by the principle of similarity. Since the peak pressure of a shock wave decreases faster than R^{-1}, a suitable theory, satisfying the principle of similarity, and accommodating this experimental observation, is desired.

An account of underwater research prior to World War II is given by Kennard (9). The advent of World War II stimulated American and British investigators (10). Shortly after World War II, the theoretical and experimental work in this field was drawn together by Cole (11). Several theories were introduced to explain shock-wave propagation in water: Penney (1940), Penney-Dasgupta (1942), Kirkwood-Bethe (1942), Kirkwood-Brinkley (1944), and Osborne-Taylor (1944).

In this study the asymptotic form of the Kirkwood-Bethe theory (12) is used because most work is compared to it. This theory in general treats: (a) the specification of the initial conditions at the water-explosion gas interface, (b) the theory of propagation of a spherical shock wave in water, and (c) the motion of the subsequent gas bubble. The asymptotic form of the Kirkwood-Bethe theory leads to an expression for peak pressure of the form:

$$p_m \sim \frac{a_0}{R}\left[\ln\left(\frac{R}{a_0}\right)\right]^{-1/2} \tag{2}$$

where a_0 is the explosive-charge radius.

In general this theory is based upon the formalism of the fundamental equations of hydrodynamics. It does explicitly satisfy the principle of similarity. Finally, it can be applied easily to a wide variety of explosives (a consideration which affects only the initial conditions).

Purpose of Report

A review of the literature reveals no studies that have been made to determine if any similarity exists between CUE and EWP events. The purpose of this report, therefore, is to determine if such similarity exists and what the scaling factors are.

DISCUSSION

In this section the techniques by which the data are interpreted are discussed, and the basic assumptions used throughout the study are specified. These specific considerations are: (a) a correction factor for the instrument response to the short-duration shock wave, (b) the energy dissipated at the spark-gap switch, (c) energy required for complete vaporization of the wire, and (d) the electrical energy expressed in terms of the equivalent TNT weight. These four items are considered in sequence below.

Duhamel's Theorem

Usually, for large-amplitude chemical explosions, the response of the detecting instrument is of nominal interest, because the explosion-time parameter τ_e is large compared to the response time of the instrument τ_a (Eqs. 4 and 5). For shock waves of small duration, however, the variation of pressure with time can be appreciable when compared to the response time of the detection system. The result of this situation is an "apparent" but untrue pressure-time profile. To accommodate this nonideal situation, a mathematical technique is utilized to correct for the physical shortcomings of the detection system. This technique is known as Duhamel's theorem (13), or the superposition theorem.

Generally the performance of a system may be determined not only by its response to a unit step function, but also by its response to an arbitrary function. These are related (in the notation of this report) by the theorem of Duhamel:

$$h(t) = p(0)A(t) + \int_{\lambda=0}^{\lambda=t} p'(\lambda)A(t-\lambda)\,d\lambda \tag{3}$$

where $h(t)$ is the oscilloscope output response in volts to an arbitrary function $p(t)$, the incident pressure wave. Here $p(0)$ is $p(t)$ at $t=0$, λ is a dummy variable, $A(t)$ is the response of the oscilloscope plus associated components in volts to a unit step function of pressure, and $h(t)$ is an experimentally measured quantity (*i.e.*, the trace on the crt in volts as a function of time). The character of $p(t)$ and $A(t)$ depend upon the amount and type of explosive and on the details of the detection system, respectively.

Equation (3) generally indicates that if $A(t)$ is expressed analytically in terms of parameters such as electric current or mechanical "time constants," and if $h(t)$ is also approximated by some parameters, then $p(t)$ can be solved analytically by using Eq. (3) in principle by means of the Laplace transform. On the other hand, if $A(t)$ and $h(t)$ are given in tabular form, then $p(t)$ can be solved numerically, as outlined by Osborne (14). The solution to Eq. (3) by either method yields a factor which is used to correct the observed first peak voltage on the oscillogram to the peak pressure in the shock wave. This peak pressure is frequently the quantity of greatest interest; therefore, let us assume for the sake of simplicity that the pressure due to the shock wave at a point is reasonably described as

$$p(t) = \begin{cases} 0 & \text{for } t \leq 0 \\ p_m e^{-t/\tau_e} & \text{for } t \geq 0 \end{cases} \tag{4}$$

and that $A(t)$, the total instrument response, is approximated by

$$A(t) = \begin{cases} 0 & \text{for } t < 0 \\ A_\infty(1 - e^{-t/\tau_a}) & \text{for } t \geq 0. \end{cases} \tag{5}$$

Substitution into and integration of Eq. (3) using these definitions yields the expression

$$h(t) = p_m A_\infty \left(\frac{\tau_e}{\tau_e - \tau_a}\right)\left(e^{-t/\tau_e} - e^{-t/\tau_a}\right). \tag{6}$$

Of course, p_m is the peak pressure of the shock wave in pounds per square inch and A_∞ is the maximum static ($t = \infty$) constant in volts per pound per square inch of the oscilloscope, including the pressure gage and amplifier system. The time at which $h(t)$ becomes a maximum value is

$$t_{max} = \left(\frac{\tau_a \tau_e}{\tau_e - \tau_a}\right) \ln \left(\frac{\tau_e}{\tau_a}\right). \tag{7}$$

The data of this report indicate that τ_e and τ_a are of the same order of magnitude. For this case, if τ_e lies between $1/2(\tau_a)$ and $3/2(\tau_a)$, Eq. (7) can be approximated by the expression

$$t_{max} \simeq \frac{1}{2}(\tau_a + \tau_e). \tag{8}$$

Thus, when the response time of the detection system (oscilloscope, amplifier, and pressure gage) to a step function of pressure is of the same order of magnitude as the decay time of the explosion wave, the observed time of rise to peak voltage on the crt is approximately equal to the decay time of the actual (or hypothesized) explosion wave. The value of $h(t)$ at its maximum point is given by substituting Eq. (7) into Eq. (6), which yields

$$h(t)_{max} = p_m A_\infty \left\{\left(\frac{\tau_e}{\tau_e - \tau_a}\right)\left[\exp^{-(\tau_a/(\tau_e-\tau_a))\ln(\tau_e/\tau_a)} - \exp^{-(\tau_e/(\tau_e-\tau_a))\ln(\tau_e/\tau_a)}\right]\right\}. \tag{9}$$

As a result, a measured peak deflection, $h(t)_{max}$ in volts, on an oscillogram under these conditions may be corrected to yield the true peak shock-wave pressure in pounds per square inch by

$$p_m = \frac{h(t)_{max}}{A_\infty \left\{\left(\frac{\tau_e}{\tau_e - \tau_a}\right)\left[\exp^{-(\tau_a/\tau_e-\tau_a)\ln(\tau_e/\tau_a)} - \exp^{-(\tau_e/\tau_e-\tau_a)\ln(\tau_e/\tau_a)}\right]\right\}}. \tag{10}$$

If p_m^* is defined as $h(t)_{max}/A_\infty$, then Eq. (10) may be written

$$p_m = \frac{p_m^*}{\left(\frac{\tau_e}{\tau_e - \tau_a}\right)\left[\exp^{-(\tau_a/\tau_e-\tau_a)\ln(\tau_e/\tau_a)} - \exp^{-(\tau_e/\tau_e-\tau_a)\ln(\tau_e/\tau_a)}\right]}. \tag{11}$$

To the extent to which Eqs. (4) and (5) are reasonable approximations, so far as peak-pressure measurements are concerned, the comparatively slow response of the detection system to a rapidly varying, short-duration pressure wave is overcome. Equations (8) and (10) give the principal explosion-wave parameters of interest, p_m^* and τ_e, directly from the observed oscillogram trace, $h(t)$. The quantity p_m^* may be thought of as a peak pressure taken from the maximum oscillogram deflection, uncorrected for the finite response time of the apparatus.

Circuit Switch Loss

According to Moses and Korneff in a recent paper (4a), an air-gap switch produces an initial current slope of zero and inhibits the current rise in the wire to a value less than that predicted by circuit theory during the first quarter cycle. Their study shows that approximately 35 percent of the initial stored energy of the capacitor is dissipated by the switch during the first half cycle of the discharge. Electrical energies, assuming no circuit loss, are designated E, where E is the total energy of the capacitor; electrical energies accounting for circuit losses and subsequent assumptions are designated E_{corr}.

Energy Required to Heat Wire

Energy is required to vaporize completely (an assumption) the wire. This energy requirement is taken into account by Vaughan (15) using the handbook values of the thermodynamic properties of the element by the general expression

$$E_v = kLD^2 \tag{12}$$

where E_v is the vaporization energy in joules, k is a material-dependent constant, L is the length of the wire in inches, and D is the wire diameter in mils. For Nichrome wire (used throughout this study), $k = 0.572$ in.$^{-1}$ mils^{-2} joules[1]. The energy assumed required for complete vaporization of half-inch-long, five-mil-diameter Nichrome wire is estimated from Eq. (12) to be a constant: ten joules.

Weight Equivalence of Electrical Energy

The electrical energy initially stored in the capacitor may be expressed in terms of an equivalent weight of TNT by means of the heat of detonation. For TNT, Price (16) indicates the calorimetric heat of detonation to be 1013 calories per gram. Consequently, the equivalent weight W in micropounds is

$$W = 525\left(\frac{0.325\,CV_0^2 - E_v}{H_D}\right) \tag{13}$$

where C is the capacitance in farads, V_0 is the initial voltage in volts to which the capacitor is charged, E_v is estimated energy in joules required to vaporize the wire completely, and H_D is the heat of detonation of TNT in calories per gram. The equivalent weight W also includes the circuit loss of 35 percent at the spark-gap switch.

EXPERIMENTAL ARRANGEMENT

Equipment

The equipment employed in this study is divided, according to its use, into three general systems: (a) a charging circuit, (b) a discharge circuit, and (c) a detection system. A discussion of the operation of this equipment follows a brief description of each system, and its arrangement is shown in Fig. 1.

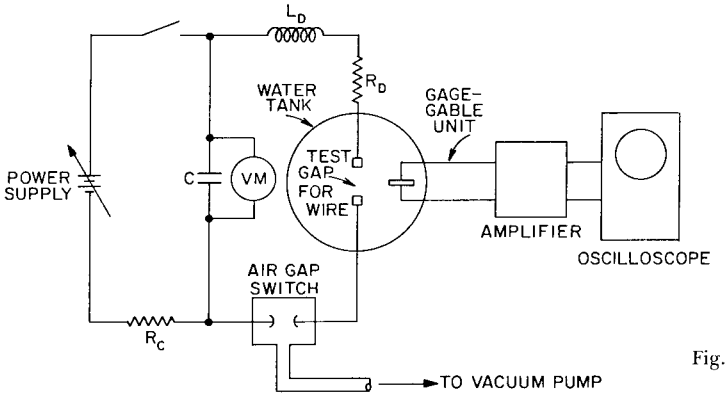

Fig. 1 — Schematic diagram of the experimental arrangement

Fig. 2 — The Axel capacitor (1/2 μf)

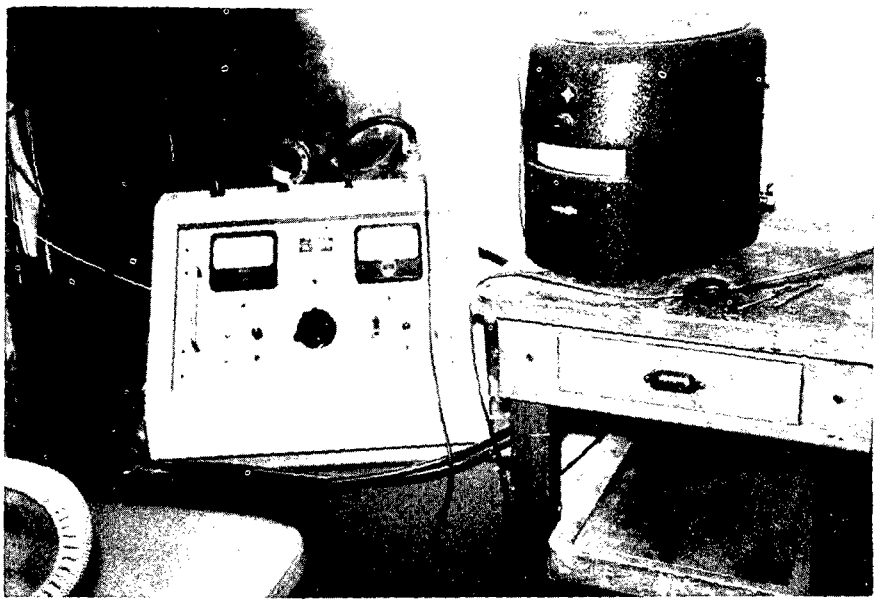

Fig. 3 — The power supply (left) and voltmeter (right)

The series charging circuit consists of the following components: (a) a power supply, (b) a charging resistor, (c) a low-inductance capacitor, and (d) a voltmeter placed in parallel with the capacitor. The energy stored in the capacitor is determined by the voltage to which it is charged by the power supply (Figs. 2, 3).

The discharge circuit is a series LRC circuit consisting of the following components: (a) the low-inductance capacitor, (b) a special air-gap switch (17), (c) electrodes, (d) vacuum pump, and (e) four low-inductance leads from the spark-gap switch to the electrodes (Fig. 4). The dielectric strength of the electrical cable is sufficient to withstand 50,000 volts.

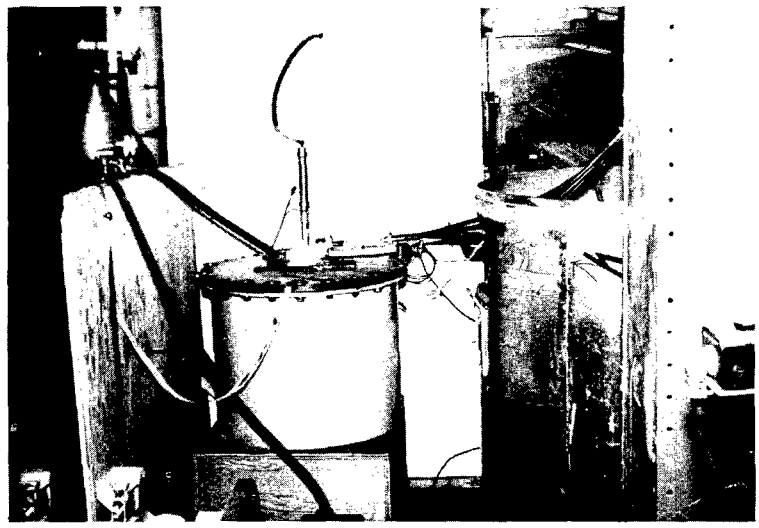

Fig. 4 — The discharge circuit (vacuum pump below capacitor, not shown)

The detection system consists of the following components: (a) an oscilloscope, (b) an oscilloscope camera, (c) an oscilloscope plug-in amplifier, and (d) a tourmaline pressure gage.

Methods

Operation of the discharge circuit is restricted to 20,000 volts, since breakdown at the air-gap switch occurs at 23,000 volts at atmospheric pressure. When the capacitor is charged to some voltage (V_0), the electrical energy stored in the capacitor may be switched through the LRC circuit by evacuating the spark-gap switch with the vacuum pump. The current passes through the low-inductance leads to the electrodes in the water tank, and back to the capacitor.

The capacitance of the low-inductance capacitor was measured by an impedance bridge to be 0.507 ± 0.001 μf. The internal inductance was stated by the manufacturer to be 60 millimicrohenries. The ringing frequency of the circuit was observed to be about 400 kc, and the circuit inductance was 0.31 microhenry. The circuit resistance was 0.05 ohm. Evaluation of circuit parameters required the use of oscillograms, and the analytic technique was adopted from Page (18). The time required for the current oscillations to damp out was about 25 μsec when the test gap was shorted with a copper bar.

The sweep speed of the oscilloscope was kept constant at five microseconds per centimeter throughout the study. The time count was initiated at the oscilloscope by placing a pickup loop near the spark-gap switch. When the discharge began, a voltage was induced in the loop, and scope time was counted from that instant. Because the transit time of the shock wave from the exploding wire to the pressure gage varied due to the variation of the gage distance, a time delay was employed on the oscilloscope in order to present the interval in which the shock wave passed by the gage. The value of the time delay, of course, depended upon the distance between the gage and the wire. The sweep time was calibrated by means of a time-mark generator.

The presentation of the pressure-time history of the shock wave on the crt of the oscilloscope was recorded by the Polaroid oscilloscope camera. Each oscillogram was then enlarged, and a tracing of each enlargement was made. From these enlargements, measurements of shock-wave parameters (amplitude and time) were made.

The differential amplifier was used to exclude some extraneous electromagnetic signals. The rise time of the oscilloscope and the amplifier as a unit was about 0.2 μsec (manufacturer's data). The amplifier was calibrated for each setting used (vertical scale 0.5 volt/cm, 1 volt/cm, and 2 volts/cm by using four or five known signals). The amplifier response was

in error by a linear factor. The measured pressures in Eq. (15) were corrected for the amplifier's error.

The pressure gage used in this study was a commercially available,* 1/4-in.-diameter, 4-ply, underwater type, tourmaline pressure gage. The design, use, and performance of such gages have been studied by Arons and Cole (19), and also by Fox, *et al.* (20). The unit was mounted on 16 ft of shielded cable which terminated directly at the amplifier input. The manufacturer's crystal constant (hydrostatically determined) was 1.99×10^{-12} coulomb/psi. The gage was employed in an edge-on position to the exploding wire. The capacitance of the gage-cable unit was 423.7 ± 0.1 $\mu\mu$f. The impedance for the feed-cable length was 69 ohms. Based upon these figures, the estimated delay time for the feed cable was about 29 nanoseconds, not a source of concern in this experiment.

To insure that the gage was watertight, a thin coat of C-276† was applied. X-ray photographs of the gage in the modified configuration indicate that the coating was 0.5 mm thick in front of the edge-on position. Moreover, the diameter of the gage was measured to be 7.65 mm.

To insure that the gage-cable unit was functioning properly after the exploding-wire experiment, calibration and field tests were performed at the Naval Propellant Plant by Slifko.‡ The gage-cable unit was calibrated by the bursting-diaphragm method which, in the modified form, yielded a crystal constant of 2.13×10^{-12} coulombs/psi, checking to within 7 percent of the manufacturer's value. In addition, tests of the gage in the edge-on position were conducted using standard Army Engineer detonator caps (about a millipound of TNT). These tests indicated that the gage performed in a satisfactory manner, one test is compared to an EWP event in Fig. 5. Actually, the rise time for the gage was a microsecond faster than other gages against which it was compared (*i.e.*, about four as compared to five microseconds). The pressure measurements were corrected to reflect the gage constant.

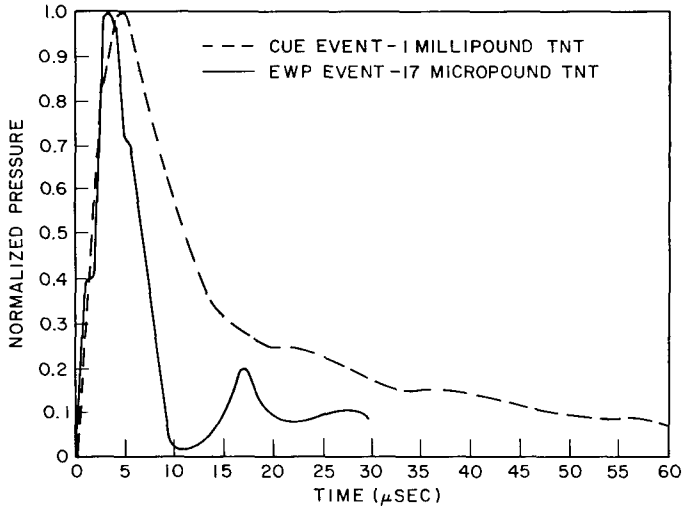

Fig. 5 — Comparison of a CUE and underwater EWP event using normalized pressure *versus* time. CUE data courtesy of John P. Slifko, NOL Unit, Indian Head, Md.

*Crystal Research, Inc., Cambridge, Mass.
†Zophar Mills, Brooklyn, N.Y.
‡John P. Slifko, NOL Unit, Naval Propellant Plant, Indian Head, Md.

Based upon the previous discussion, the voltage (vertical deflection) measured from the oscillogram is given by Cole (11a) as

$$V = \left(\frac{KA}{C_0 + C_1}\right) p_m^* \tag{14}$$

where V is the voltage in volts, KA is the crystal constant in micromicrocoulombs/psi, C_0 is the lumped capacitance of the cable-gage unit in micromicrofarads, C_1 is the input capacitance of the amplifier in micromicrofarads, and p_m^* is the peak pressure in psi uncorrected by Duhamel's theorem. Since the only quantity undetermined is p_m^*, the value of p_m^* is, for $C_0 = 424$ $\mu\mu$f, $C_1 = 45$ $\mu\mu$f, and $KA = 2.13$ $\mu\mu$c/psi:

$$p_m^* \text{ (psi)} = 220 \text{ v.} \tag{15}$$

Equation (15) does not reflect the correction required for the linear amplifier error nor due to the system response (Eq. 10).

The distance between the pressure gage and the exploding wire was varied from 1.5 to 12.0 in.; measurements were taken every 1.5 in. Because the distances involved were small, and because accurately positioning the gage was not possible, accurate distance measurements were difficult to make. The actual distance was always less than the measured distance by as much as 0.200 in. due to the technique of mounting the wire and measuring the distance.

DATA AND RESULTS

The data used in this study are obtained from oscillograms which give, directly, the voltage deflection from a reference position on a crt as a function of time. The voltage deflection results from the charge applied to the plates of the crt. This charge is generated by the piezoelectric effect plus the amplifier; in this case, it is due to the compression of a tourmaline gage by a shock wave. The data in this study are obtained from the use of Nichrome wire exclusively.

A comparison of EWP pressure-time profiles can be made to CUE. In Fig. 5, for example, a profile representing a CUE and one an underwater EWP event are presented to show, qualitatively, the contrast between the two types of explosions. The pressure of each is normalized for this comparison.

As mentioned before, and throughout this article for EWP data, a distinction is maintained between the peak pressure p_m^*, which is measured directly from oscillographic data, and p_m, which is calculated using p_m^* on the basis of certain time constants. The quantity p_m^* includes all corrections, calibrations, and assumptions except those given by the Duhamel theorem. The quantity p_m includes all corrections, including those given by Duhamel's theorem, *i.e.*, the denominator in Eq. (10) or(11).

Pressure Measurements

Energy Adjustments Related to Scaling Peak Pressure p_m^*—In CUE experiments, the peak pressure shows its distance dependence in the asymptotic form as

$$p_m \propto R^{-\beta_0} \tag{16}$$

where R is the gage distance and β_0 is a constant slightly greater than unity for CUE data. The peak pressure also depends upon the charge weight W. At any value of R the peak pressure is related to the weight of the charge and the gage distance R by the law of similarity:

$$p_m \propto \left(\frac{W^{1/3}}{R}\right)^{\beta_0}. \tag{17}$$

Equivalently the electrical energy of the capacitor could be related by Eq. (17) through the heat of detonation H_D to an expression involving chemical energy. A similarity curve for p_m *versus* either k_1 $(W^{1/3}/R)^{\beta_0}$ or k_2 $(E^{1/3}/R)^{\beta_0}$ is possible. The literature, however, historically uses the relation

$$p_m = k_1 \left(\frac{W^{1/3}}{R}\right)^{\beta_0} \tag{18}$$

where k_1 depends upon the type of explosive.

In Fig. 6 the average peak pressure p_m^* in arbitrary units is plotted against the cube root of the corrected (E_{corr}) and uncorrected (E) initial capacitor energy at a fixed distance. Clearly the corrected electrical-energy values form a straight line whose slope is greater than that for the acoustic-law curve. The uncorrected energy values do not form a straight line. All wires used were 5-mil-diameter, one-half-inch-long Nichrome.

Oscillographic data were taken for capacitor energies varying from 25.4 joules (10 kv) to 101.5 joules (20 kv) and for gage distances varying from 1.5 in. to 12.0 in. in increments of 1.5 in. The results of this experiment are shown for peak pressure in Fig. 7. Here the peak pressure, p_m^*, is plotted against the cube root of the equivalent weight of TNT divided by the gage distance.

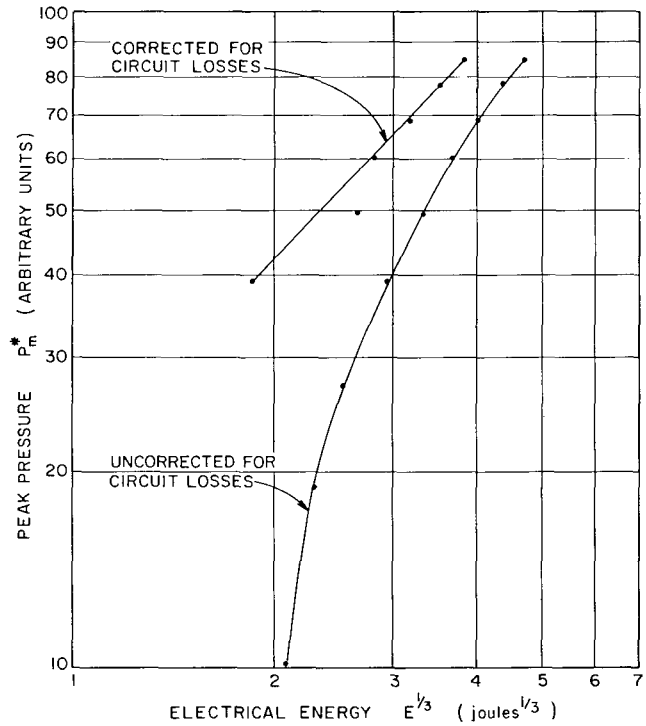

Fig. 6 — Peak pressure (uncorrected for instrument response) *versus* the cube root of the electrical energy (corrected and uncorrected for circuit losses) for Nichrome wire, 1/2 in. long, 5 mils in diameter, at a gage distance of 9 in.

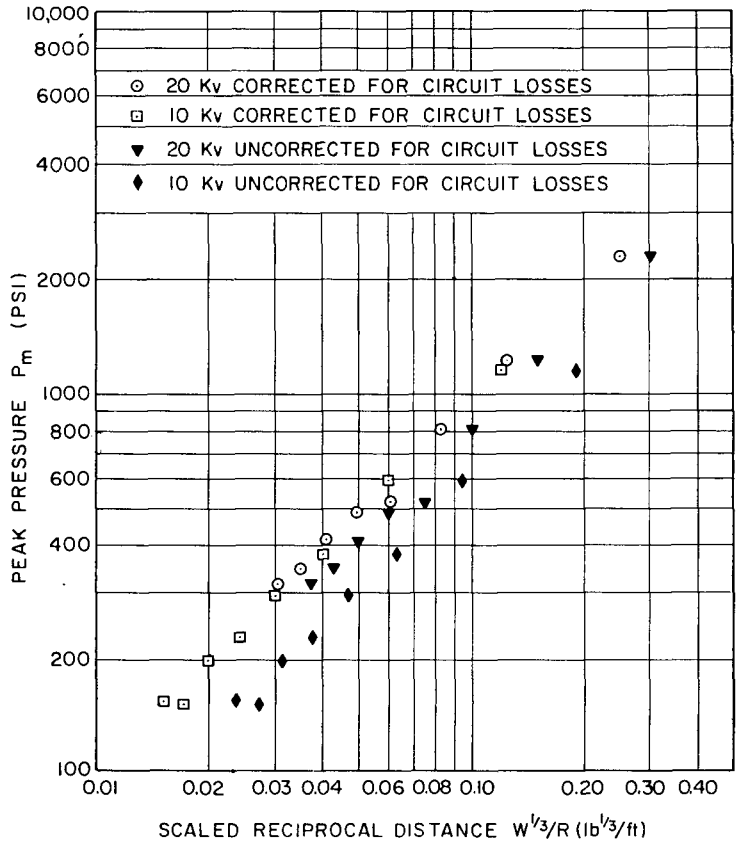

Fig. 7 — Peak pressure (uncorrected by Duhamel's theorem) *versus* scaled reciprocal distance (both for uncorrected and corrected electrical energy)

The equivalent weight of TNT is estimated for 100 percent of 1/2 CV_0^2 and for 100 percent of 1/2 CV_0^2 less the values of the circuit loss (35 percent of 1/2 CV_0^2) and wire vaporization (10 joules). These considerations are termed uncorrected (E) and corrected electrical energies (E_{corr}), respectively. The corrected data in Fig. 7, therefore, represents an expression of the form

$$p_m^* = k_3 \left(\frac{W^{1/3}}{R}\right)^{\beta_1} = k_4 \left(\frac{E^{1/3}}{R}\right)^{\beta_1} \tag{19}$$

where p_m^* here is the peak pressure uncorrected by Duhamel's theorem, k_3 is a constant of the same order of magnitude as k_2 for TNT, k_4 is a constant, E_{corr} is defined above, and β_1 is a constant slightly greater than unity for EWP data. Figure 7 contains data for the two extreme values of electrical energy only, 25.4 and 101.5 joules. Note that the data using only corrected energies form a common curve, or scale, whereas the uncorrected energies form two distinct lines having the same slope. The data for E_{corr} is chosen to represent EWP because it forms a common curve. On the basis of the information presented in Fig. 7, further comparisons are made using the corrected electrical energy values in Fig. 8.

Comparison of EWP p_m^* to CUE p_m Data—In Fig. 8 CUE and EWP data are compared. Individual CUE data points are included (see legend) from the work of several investigators. Two curves are presented relating peak pressure, p_m for CUE, and p_m^* for EWP, to the scaled reciprocal distance. Curve 1 is the asymptotic approximation of the Kirkwood-Bethe theory using TNT (density 1.59 g/cc) and is given by the empirical expression reported by Arons (24)

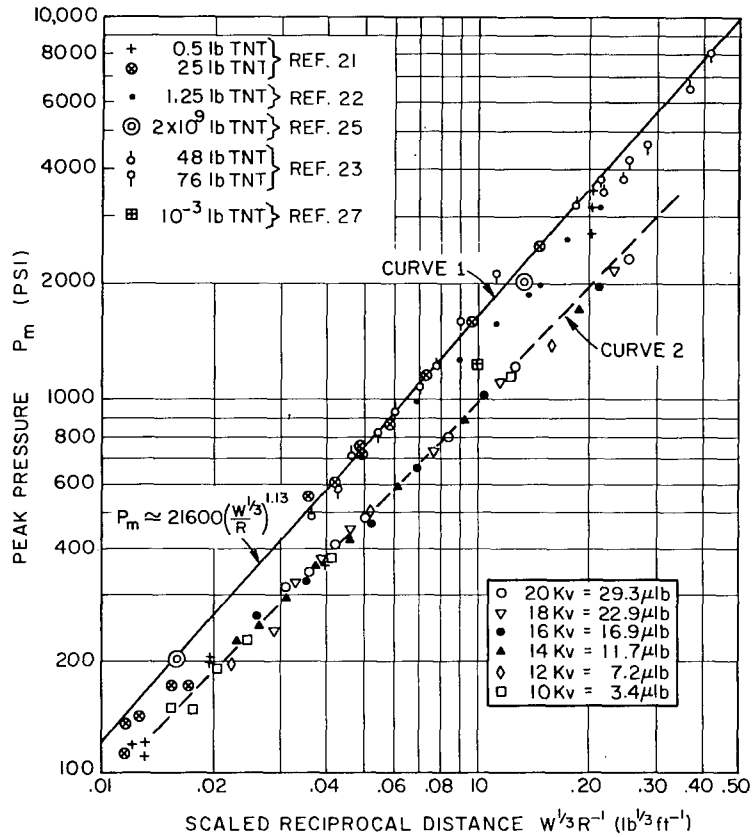

Fig. 8 — Peak pressure *versus* scaled reciprocal distance for CUE data (curve 1) and EWP data (curve 2). EWP data are uncorrected for instrument response (Duhamel's theorem)

$$p_m = 21{,}600 \left(\frac{W^{1/3}}{R}\right)^{1.13} \tag{20}$$

where W is the charge weight in pounds, R is the gage distance in feet, and p_m is the peak pressure in pounds per square inch for CUE events. This curve is drawn from data using 55, 25, and 0.5 lb TNT charges. Curve 2 is the result of plotting all exploding-wire data (*i.e.*, 20, 18, 16, 14, 12, and 10 kv shots at distances of 1.5, 3.0, 4.5, 6.0, 7.5, 9.0, 10.5, and 12.0 in.) and adjusting each energy for the assumption of complete vaporization and for the energy dissipated at the spark-gap switch. Clearly, several statements seem to be in order upon examining Fig. 8. First, curve 2 (EWP data) is about 50 percent lower than curve 1 (TNT data) for a given value of $W^{1/3}/R$. Secondly, on the basis of Fig. 8 the corrected EWP data seems to form a similarity curve not unlike TNT data. Thirdly, the slope of curve 2 seems to be less than 1.13, as in TNT data, but also is no less than unity. Curve 2 of Fig. 8 supports the conclusion that the peak pressure at least of EWP scales like a chemical explosion in general, when the electrical energy is corrected for circuit and evaporation requirements.

The weight of an equivalent TNT charge for EWP is calculated to be

$$W \text{ (micropound)} = 525 \left(\frac{0.325\, CV_0^2 - E_v}{H_D}\right). \tag{21}$$

If this equivalent weight of TNT is cast into spherical form, its radius a_0 in inches is given by

$$a_0 \text{ (in.)} = 0.0394[(E_{corr})]^{1/3} \tag{22}$$

where E_{corr} is the corrected electrical energy in joules.

For voltages less than 10 kv (25.4 joules), the basic assumption of complete vaporization tends to be less believable because there would be very little energy left for the shock wave if a constant 10 joules is used to vaporize the wire.

The essential pressure and time data for all shots of this study are presented in Table 1. Column 1 of Table 1 identifies the particular shot, column 2 lists the voltage in kilovolts, and column 3 lists the gage distance in inches. Column 4 lists the peak pressure p_m^* in volts. Column 5 presents the peak pressure p_m^* in psi, calculated from Eq. (15). The crystal constant as determined by Slifko, $KA = 2.3\ \mu\mu$ coul/psi, is used here. Columns 6 and 7 are explained later in this report.

Comparison of EWP (p_m) to CUE (p_m) Data—Based upon the values of t_m and the value of τ_a, the maximum value of p_m may be calculated from Eq. (10). Equation (10) varies little if individual values of t_m are not greatly different. The result is nearly a constant, *i.e.*, $p_m = p_m^*/0.43$. Therefore, the oscillographic pressure values may be corrected by multiplying each by the factor 2.32. These values are presented in column 6 of Table 1 and are also compared to CUE theory and data (24) and to a one-megaton nuclear weapon (25) in Fig. 9. Column 7 of Table 1 presents the values of scaled reciprocal distance based upon the equivalent weights W of TNT corresponding to the corrected initial capacitor energy (E_{corr}). Figure 9 indicates that EWP pressure data are approximately 40 percent larger than CUE data for the same value of $W^{1/3}/R$ and can be described approximately by the expression:

$$p_m = 26{,}800 \left(\frac{W^{1/3}}{R}\right)^{1.08} \tag{23}$$

Conversion From Electrical to Shock-Wave Energy

The energy of a shock wave propagating under water is given approximately by Cole (11b):

$$W(R) = \frac{4\pi R^2}{\rho_0 C_0} \int_{t(R)}^{\tau} [p(t)]^2\, dt. \tag{24}$$

The calculations are presented in Fig. 10 for energies ranging from 25.4 joules (10 kv) to 101.5 joules (20 kv) at a constant distance, $R = 1.5$ in. In this figure the ratio of shock-wave energy to initial stored electrical energy in percent is plotted against the initial stored capacitor voltage. The percentage ranges from 51 to 62 percent and has an average value of 58.0 percent. Bennett (26) using 4 and 5 mil copper wires, at energies ranging from 20 to 37 joules, indicates that approximately 40 to 60 percent of the initially stored electrical energy is deposited in the wire and is available for subsequent fluid motion. Buntzen (4b), using 5-mil, one-inch-long copper wires, exploded underwater, finds the shock-wave energy about 63 percent of that initially stored in the capacitor. The energy-conversion factor determined in this study shows reasonable agreement with the independent results of these investigators, *i.e.*, an average value of 58.2 percent approximately.

Time Measurements

Time Constant of Underwater EWP Events—In general, a comparison of time measurements for CUE and EWP events show that the explosion time constant is smaller by a factor of 10^3 in general for EWP. In most CUE experiments, for example, the decay time constant is expressed in milliseconds. In this study, however, a measurement of only a few microseconds is observed.

TABLE 1
Pressure and Distance Data for
Underwater Exploding Nichrome Wires

Shot No.	Voltage (kv)	R (in.)	p_m^* (volts)	p_m^* (psi)	p_m (psi)	$W^{1/3}/R$ ($lb^{1/3}/ft$)
1	20	1.5	8.70	2297	5329	0.2472
2	18		8.20	2165	5023	0.2272
3	16		7.36	1943	4508	0.2056
4	14		6.42	1694	3930	0.1816
5	12		5.32	1404	3257	0.1544
6	10		4.10	1100	2552	0.1208
7	20	3.0	4.5	1198	2779	0.1236
8	18		4.16	1107	2568	0.1136
9	16		3.76	1009	2341	0.1028
10	14		3.26	875	2030	0.0908
11	12		2.76	747	1733	0.0772
12	10		2.10	578	1341	0.0604
13	20	4.5	2.98	794	1842	0.0824
14	18		2.75	726	1684	0.0757
15	16		2.50	660	1531	0.0685
16	14		2.20	581	1348	0.0605
17	12		1.88	501	1161	0.0515
18	10		1.40	376	872	0.0403
19	20	6.0	1.94	517	1199	0.0618
20	18		1.97	485	1125	0.0568
21	16		1.87	464	1077	0.0514
22	14		1.68	418	970	0.0454
23	12		1.43	356	826	0.0386
24	10		1.12	280	650	0.0302
25	20	7.5	1.92	481	1116	0.0494
26	18		1.79	449	1041	0.0454
27	16		1.62	406	942	0.0411
28	14		1.41	353	819	0.0363
29	12		1.20	304	705	0.0309
30	10		0.88	223	517	0.0242
31	20	9.0	1.62	406	942	0.0412
32	18		1.48	372	863	0.0379
33	16		1.30	326	756	0.0343
34	14		1.16	291	675	0.0303
35	12		1.00	253	587	0.0257
36	10		0.75	191	443	0.0201
37	20	10.5	1.39	342	793	0.0353
38	18		1.25	314	728	0.0325
39	16		1.13	286	664	0.0294
40	14		0.97	245	568	0.0259
41	12		0.77	196	455	0.0221
42	10		0.58	150	348	0.0173

(Table Continues)

TABLE 1 (Continued)
Pressure and Distance Data for
Underwater Exploding Nichrome Wires

Shot No.	Voltage (kv)	R (in.)	p_m^* (volts)	p_m^* (psi)	p_m (psi)	$W^{1/3}/R$ ($lb^{1/3}/ft$)
43	20	12.0	1.25	314	729	0.0309
44	18		1.14	289	671	0.0284
45	16		1.04	263	610	0.0257
46	14		0.89	225	522	0.0227
47	12		0.75	191	443	0.0193
48	10		0.59	152	353	0.0151

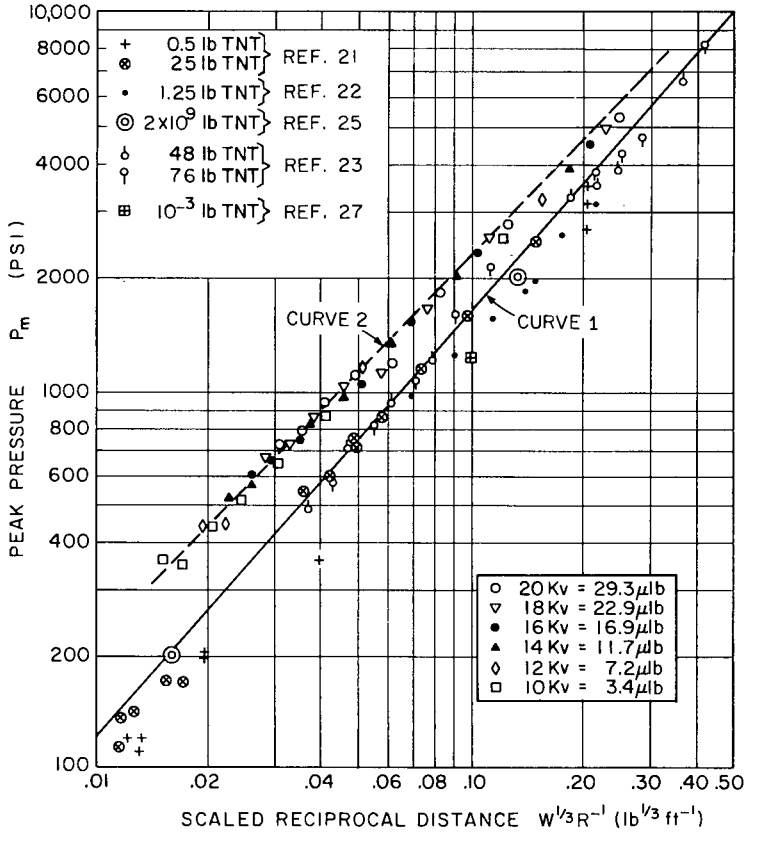

Fig. 9 — Comparison of CUE (curve 1) and EWP (curve 2) data using peak pressure and scaled reciprocal distance. EWP data are corrected for instrument response.

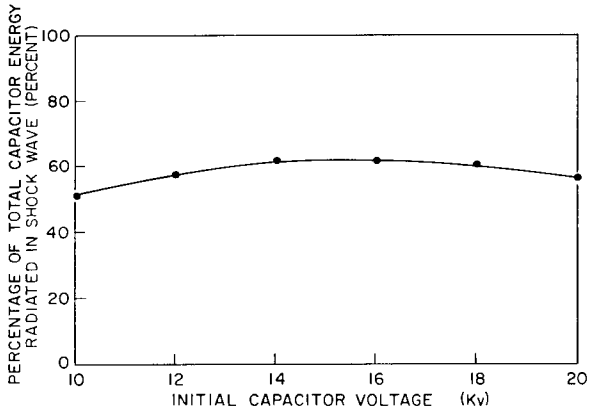

Fig. 10 — Ratio of shock-wave energy to initial capacitor energy *versus* initial capacitor voltage

Definition of τ_e for EWP Events—For large-amplitude CUE events, the pressure behaves approximately as $p(t) = p_0\, e^{-t/\tau}e$, and the explosion constant τ_e is evaluated over the range where the disturbance has fallen to $(1 - e^{-1})$ of its maximum value. On a semilog plot of peak pressure *versus* time, τ_e is the slope (in milliseconds) which is a constant over the range of p_m to approximately $0.67p_m$.

The small-amplitude explosions of this study (EWP), on the other hand, do not lend themselves to such an analysis. The rise of the pressure wave to a maximum value does not behave like a step function of pressure which then decays exponentially. Moreover, the pressure decays almost as rapidly as it rises to a maximum. If the definition of the explosion constant for large-duration explosions is used for the small-duration waves in this study, then points on the oscillographic record are chosen in every instance in the situation where the explosion wave has not entirely crossed the crystal area. The explosion time constant defined for EWP and for this study is approximated by Eq. (8) and is defined as the average value of time over which this approximate expression is valid (*i.e.*, $t_{max} \simeq 1/2(\tau_a + \tau_e)$.

Definition and Calculation of τ_a for EWP Events—The quantity τ_a, as expressed in Eq. (5), for the amplifier alone, excluding the gage, is about 0.2 μsec. A further consideration is that the crt cannot display a voltage deflection from its reference position until the tourmaline gage has been sufficiently compressed. Consequently, the transit time required for the explosion wave to compress the gage sufficiently must be taken into account. The transit time is defined here to be the time required for the explosion wave to traverse $(1 - e^{-1})$ of the diameter normal to the explosion wave. From x-ray photographs, d is measured to be 7.65 mm. The time interval for the explosion wave to traverse the distance $(1 - e^{-1})\, d$ is estimated to be: (0.765) (0.63)/ $0.15 \times 10^6 = 3.21$ μsec. The combined characteristic time constant for the gage-amplifier-oscilloscope system is calculated to be, therefore, $3.21 + 0.20 = 3.41$ μsec $= \tau_a$.

Time Measurements of EWP Shock Wave Profiles—Measurements of the partial rise time θ_1, as shown in Fig. 11, and of subsequent time intervals corresponding to $p = 0.5\ p_{max}$ (*i.e.*, θ_2, and θ_3 and to $p = 0.25\ p_{max}$ (*i.e.*, θ_4 and θ_5) have been taken. The average value for all θ_1 measurements is 2.07 μsec, for t_{max} is 3.42 μsec, for θ_2 is 3.12 μsec, for θ_3 is 5.08 μsec, for θ_4 is 4.15 μsec, and for θ_5 is 6.92 μsec. These values are obtained from Table 2, which gives all time measurements.

Comparison of $(\tau_e)_{calc}$ With $(\tau_e)_{exp}$—As stated before, $\tau_e = 2t_{max} - \tau_a$. The calculated value of τ_a is 3.41 μsec. The measured average value of t_{max} is 3.42 μsec. This measure of agreement gives some confidence to the assumption that $\tau_e = 2\tau_{max} - \tau_a$ and to the consequences of Eq. (10) or (11).

Increasing Value of τ_e With Propagation—Arons (24) has shown evidence that τ_e for large-amplitude shock waves increases in value with propagation distance for charge weights varying

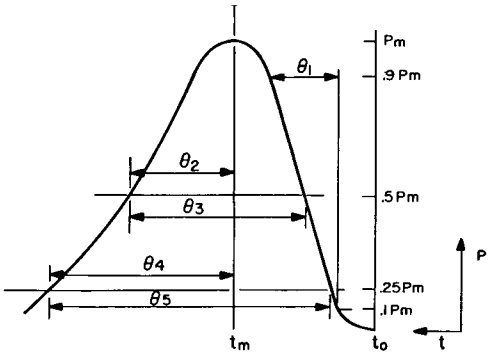

Fig. 11 — The form of an ideal oscillographic record, indicating the various time measurements

TABLE 2
Time Measurements from Oscillographic Records

Shot No.	Voltage (kv)	R (in.)	θ_1 (μsec)	θ_2 (μsec)	θ_3 (μsec)	θ_4 (μsec)	θ_5 (μsec)	t_{max} (μsec)
43	20	12.0	2.41	2.72	5.17	3.79	7.33	4.57
37		10.5	2.50	2.76	5.52	3.88	7.41	4.22
31		9.0	2.33	2.85	5.43	3.88	7.24	—
25		7.5	2.41	2.76	5.43	3.79	7.24	4.22
19		6.0	2.38	2.93	5.52	4.05	7.33	4.05
13		4.5	2.07	3.02	5.17	4.14	6.98	3.45
7		3.0	2.16	3.10	5.00	4.22	6.72	3.19
1		1.5	1.72	3.45	5.26	4.40	6.72	2.93
44	18	12.0	2.30	2.78	5.38	4.03	7.49	3.97
38		10.5	2.21	2.98	5.47	4.03	7.39	3.79
32		9.0	1.92	2.78	5.57	3.84	7.30	3.79
20		6.0	2.02	3.46	5.18	4.22	6.72	2.93
14		4.5	2.02	3.36	4.99	4.42	6.91	2.93
8		3.0	2.11	3.07	4.99	4.13	6.91	3.19
2		1.5	1.82	3.26	4.80	4.42	6.82	2.59
45	16	12.0	1.99	2.74	5.58	3.69	7.28	4.33
39		10.5	2.17	2.55	5.10	3.59	6.99	4.23
33		9.0	2.08	2.65	5.29	3.69	7.18	4.13
27		7.5	1.99	3.59	5.20	4.63	7.18	3.46
21		6.0	1.99	3.40	5.10	4.44	6.90	3.17
15		4.5	2.08	3.40	5.10	4.35	6.99	3.46
9		3.0	2.08	2.27	4.82	4.16	6.62	3.26
3		1.5	1.89	3.12	4.73	4.25	6.62	3.08
46	14	12.0	2.21	3.46	5.38	4.42	7.20	—
40		10.5	2.21	3.36	5.18	4.32	6.91	—
34		9.0	2.11	3.36	5.09	4.22	6.91	3.46
28		7.5	2.02	3.46	5.38	4.42	7.20	3.46
22		6.0	1.82	3.36	5.09	4.42	6.91	3.08
16		4.5	2.02	3.17	4.80	4.32	6.82	3.27
10		3.0	1.92	3.36	5.09	4.32	6.82	3.17
4		1.5	1.92	2.98	4.61	4.03	6.53	3.17

(Table Continues)

TABLE 2 (Continued)
Time Measurements from Oscillographic Records

Shot No.	Voltage (kv)	R (in.)	θ_1 (μsec)	θ_2 (μsec)	θ_3 (μsec)	θ_4 (μsec)	θ_5 (μsec)	t_{max} (μsec)
47	12	12.0	2.08	—	—	—	—	—
41		10.5	2.17	3.31	4.91	4.25	6.80	3.30
35		9.0	1.99	3.50	5.10	4.44	6.90	3.21
23		6.0	1.99	3.21	4.82	4.25	6.71	3.02
17		4.5	2.08	3.02	4.73	3.97	6.52	3.30
11		3.0	—	—	—	—	—	—
5		1.5	1.99	3.02	4.44	3.97	6.43	3.11
48	10	12.0	1.98	3.36	5.00	4.22	6.72	3.16
42		10.5	1.98	3.24	4.83	4.22	6.72	3.16
36		9.0	2.07	3.36	5.00	4.31	6.81	3.25
30		7.5	1.99	3.53	5.00	4.40	6.64	2.98
24		6.0	1.90	3.16	4.66	4.14	6.52	3.07
18		4.5	1.98	3.10	4.74	4.14	6.50	3.16
12		3.0	2.16	2.93	4.48	3.88	6.26	3.16

$$\bar{\theta}_n = \frac{\sum_{i=1} (\theta_n)_i}{j}$$

$\bar{\theta}_1 = 2.07$ μsec $\quad$ $\bar{\theta}_4 = 4.15$ μsec

$\bar{\theta}_2 = 3.12$ μsec $\quad$ $\bar{\theta}_5 = 6.92$ μsec

$\bar{\theta}_3 = 5.08$ μsec $\quad$ $\bar{t}_{max} = 3.42$ μsec

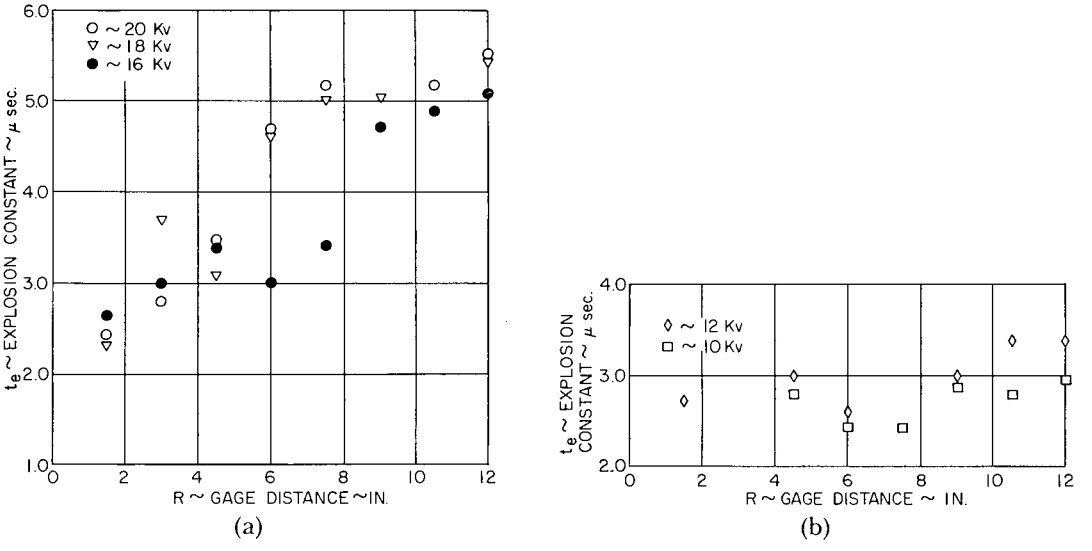

Fig. 12 — A plot of t_{max} *versus* gage distance (a) for 20, 18, 16, and 14 kv EWP explosions and (b) for 12 and 10 kv EWP explosions

from 0.5 lb to 55 lb of TNT. Osborne and Taylor (27), using a millipound of TNT, were not able to report this phenomena, although they did show a departure for the acoustic law. However, increasing τ_e (or profile broadening) for shock waves is predicted by the theory of Kirkwood and Bethe (12).

A graph of t_{max}, Figs. 12a and 12b, indicates some evidence of profile broadening with distances. Figure 12a presents t_{max} *versus* distance for 20, 18, 16, and 14 kv, while Fig. 12b presents data for 12 and 10 kv. The strongest evidence for increasing a time constant with propagation is given in the 20-kv data; the slope of the curve drawn through the points for decreasing initial electrical energy is negative. For 10-kv data it is very difficult to establish that the slope of the curve is positive. Other time measurements, except θ_5, did not show this behavior.

Comparison of Reduced Time Constants for EWP and CUE Data—The time parameter for large-amplitude CUE events scales, *i.e.*, forms a similarity curve. Figure 13 presents for CUE events the theoretical variation of the reduced time constant with the scaled reciprocal distance in curve 1, which is given by the expression

$$\frac{t}{W^{1/3}} = 9.52 \left(\frac{\frac{R}{W^{1/3}}}{\ln 10} + 0.873 \right)^{1/2} \tag{25}$$

where t is the time in microseconds, W is the charge weight in pounds, and R is the gage distance in feet. Curve 2 of Fig. 13 is based on the experimental work of Arons (34) and is given by the empirical formula

$$\frac{\theta}{W^{1/3}} = 58 \left(\frac{W^{1/3}}{R} \right)^{-0.22} \tag{26}$$

The time measurement for CUE data is θ, in microseconds, and is the time required for the pressure to drop from its maximum value to $(1 - e^{-1})$ of its maximum value (about 67 percent). The time measurement t_e for EWP data is the explosion constant ($\tau_e = 2t_{max} - \tau_a$) of the pressure wave in units of microseconds time located at the maximum of the curve.

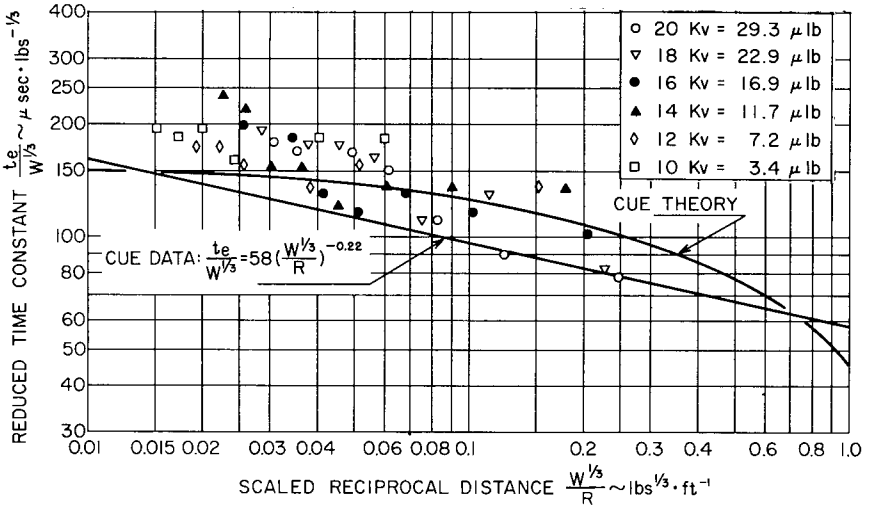

Fig. 13 — Comparison of reduced time constant *versus* scaled reciprocal distance for CUE and EWP data

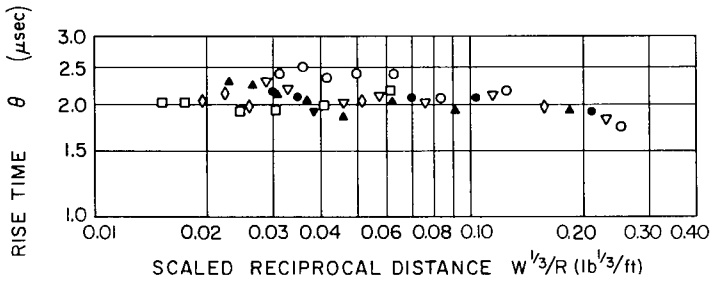

Fig. 14 — Plot of rise time *versus* scaled reciprocal distance corresponding to EWP data of Fig. 13

EWP data are presented in Fig. 13 in the form of points. The voltage (or energy) associated with each point is identified by the legend of this figure. The EWP data are obtained from t_{max} measurements. Aside from t_{max} and θ_5, the other θ measurements of Fig. 11 do not indicate a negative slope, nor do they scale. The EWP data of Fig. 13 show qualitative numerical agreement to CUE theory and CUE data. The reduced time constant for EWP does scale, however. An empirical expression relating the reduced time constant to the scaled reciprocal distance is obtained from Fig. 13.

$$\frac{\tau_e}{W^{1/3}} = 70 \left(\frac{W^{1/3}}{R}\right)^{-0.22} \tag{27}$$

EWP data do show a gentle negative slope; this suggests profile broadening (increasing t_{max} and θ_5 with distance propagation). Upon this delicate evidence, the nonlinear propagation of a small-amplitude shock wave can be inferred, since profile broadening and nonlinear propagation are inseparable constituents of shock-wave propagation (*i.e.*, one cannot occur without the other).

As a matter of interest, these results are contrasted to the work of Osborne and Taylor, who observed a departure from the acoustic law but not profile spreading. In this study no departure from the acoustic law can be claimed, but some evidence of profile spreading is observed for some time measurements.

Figure 14 also presents EWP data points of rise time associated with each data point above.

Oscillographic Data

Figure 15 represents 101.5 (20 kv) joule explosions whose oscillographic records were taken at gage distances ranging from 1.5 to 12.0 in., in 1.5-in. intervals. This set of records is representative of the entire 43 shots. Close inspection allows classification of these oscillograms according to their waveform as type A, type B, and type C, as shown in Fig. 16.

Type A Oscillograms—Type A oscillograms are, for all energies (*i.e.*, 20, 18, 16, 14, 12, and 10 kv), associated with a gage distance of 1.5 in. and sometimes 3.0 in. for higher energy explosions and are characterized by two pressure peaks. The first pressure peak is associated with the initial portion of the wire-explosion process. The second pressure peak is approximately one-quarter the amplitude of the first, occurs approximately 17 μsec after the arrival of the primary shock wave, and has a positive value of amplitude. The agency causing this secondary wave is not uniquely determined, but several possible causes can be ruled out. First, the secondary wave cannot be reflected from the water surface above, because depths of 1.0 to 3.0 in. require a time interval of 34 to 102 μsec, which is at variance with observations, and because reflections would exhibit a negative pressure, which is not observed in type A oscillographs. Secondly, the possibility of a bubble oscillation is ruled out due to the inertia of the water (production

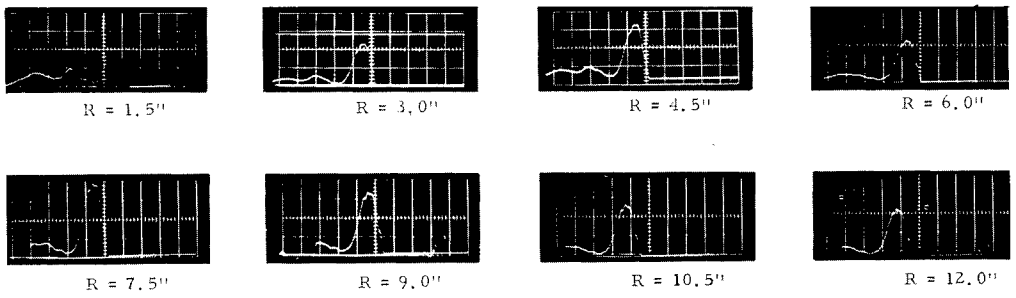

Fig. 15 — Oscillographic records for 101.5 joule EWP shots; time 5 μsec per division

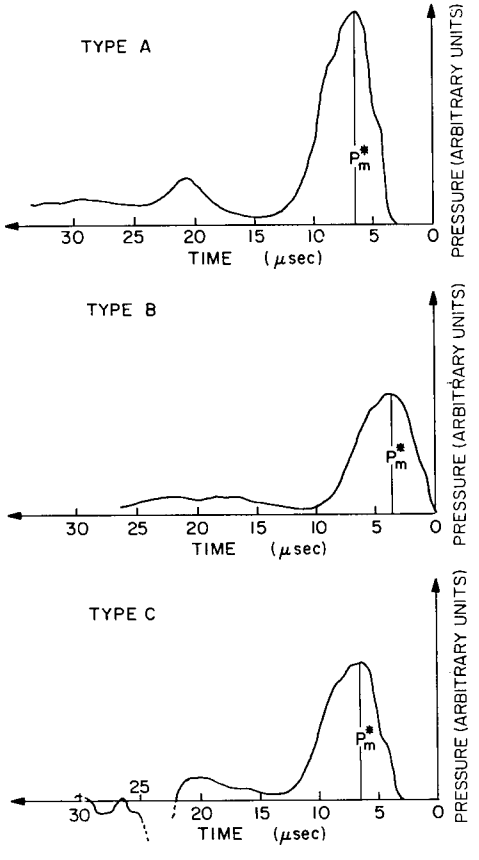

Fig. 16 — Classification of pressure-time oscillograms

of a secondary pressure wave requires time of the order of milliseconds). This is further ruled out by the experimental work of Gilstein (28), for example, using oil instead of water, which showed that bubble formation alone required several milliseconds. The most likely contributor to the secondary pressure pulse seems to be a mechanism associated with the exploding wire itself; this would be the phenomenon of restrike or reignition. When current dwell occurs during the wire explosion, a subsequent reignition and expansion of plasma (a second explosion

of the wire) take place. Further observation of the secondary shock wave at increasing values of R, due to either explanation, is obscured because, while their amplitudes are different, they propagate at approximately the same speed. To establish firmly what agency causes the secondary shock wave is not possible with the present available information; electrical measurements of the explosion process are necessary for this. This most interesting anomaly appears, however, to be atypical of CUE events and, apparently, a property of EWP events under the conditions of this experiment.

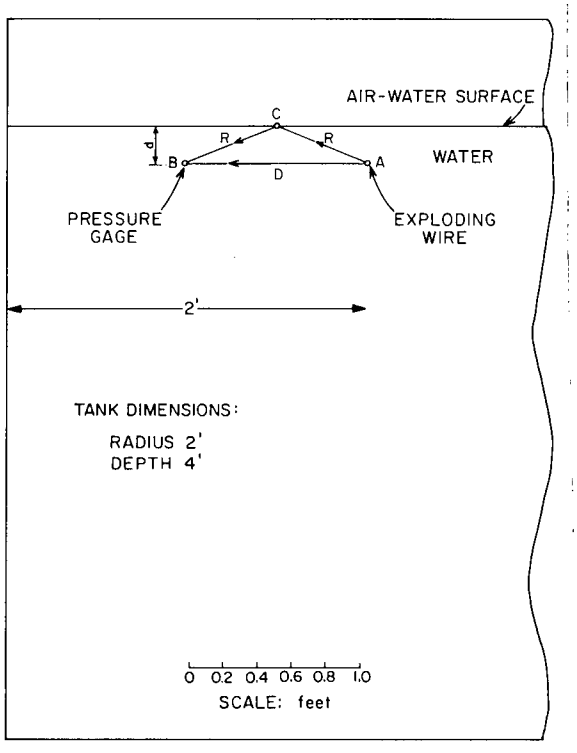

Fig. 17 – Diagram of the experiment showing the tank dimensions

Type B Oscillograms—Type B oscillograms are characterized for all energies and for distances generally of 3.0 to 7.5 in. by a primary shock wave, which falls from some peak pressure value to a random varying pressure whose amplitude ranges from 0.25 to 0.15 p_{max}.

Type C Oscillograms—Type C oscillograms are characterized for all initial energies and for distances ranging from 7.5 to 12.0 in. by a primary shock wave which decreases from some peak value, as in type B oscillograms, but which differ from type B by the inclusion of a very-well-defined, steep-slope negative pressure trace. The onset of this negative pressure varies from 10 to 23 μsec after the arrival of the primary shock wave. The cause of the negative pressure gradient appears to be the reflection of the primary shock wave from the surface of the water. The situation for EWP in this study is described in Fig. 17, where the wire is exploded at point A and a shock wave propagates outward toward point B and toward the surface of the water at point C. At point C the wave is reflected back toward point B. The time interval between the arrival of the primary shock wave at B and the onset of the negative pressure gradient depends upon the depth at which the explosion takes place. If C_0 is 1500 m/sec and d is 2 to 3 in., the time interval Δt is 10 to 23 μsec, respectively. During the course of the experiment, because

no special effort was made to keep the parameter d constant, type C oscillograms are observed for $7.5 \leq R \leq 12.0$ in. for time intervals of approximately 16 μsec. The tank dimension and depth of water below the expolsion preclude any other source for the observed negative pressure gradients. The negative pressure appears at the right time interval, given the depth, gage distance, and propagation speed of the explosion wave. These parameters are related by the simplified expression:

$$\Delta t = \left\{\frac{2D}{C_0}\left[\left(\frac{d}{D}\right)^2 + \left(\frac{1}{2}\right)^2\right]^{1/2} - 1\right\} \tag{28}$$

where Δt is the time interval following the primary shock wave of the reflected shock wave at the pressure gage in microseconds, D is the gage distance, d is the depth, and C_0 is taken as the speed of sound for purposes of approximation.

CONCLUSIONS

Based upon the measurements and analysis, several conclusions may be drawn concerning the shock-wave parameters pressure and time and their comparison to chemical explosives.

1. Peak-pressure measurements form a similarity curve only if corrections for switch losses and vaporization requirements are taken into account.

2. As a result of the first conclusion, the principle of similarity is extended in terms of charge weight six decades from pounds to micropounds for the case of peak pressure, or similarity now spans 15 decades (*i.e.*, 10^{-9} to 10^{-6} lb). A plot of peak pressure *versus* the cube root of the equivalent weight divided by the gage distance is within the same range of values given by Arons for TNT pressure data.

3. As a result of the first and second conclusion, the formula relating the total initial stored electrical energy to its equivalent weight in TNT is given by:

$$W \text{ (micropounds)} = 525\left(\frac{0.325\ CV_0^2 - E_v}{H_D}\right).$$

Here C is the capacitance in farads, V_0 is potential in volts, E_v the vaporization energy in joules, and H_D is the heat of detonation of TNT in calories per gram. This formula accounts both for the switch loss of 35 percent of the initial stored energy and for the vaporization energy (or joule heating).

4. The asymptotic formula for peak pressure for EWP data is:

$$p_m = 26{,}800\left(\frac{W^{1/3}}{R}\right)^{1.08}$$

5. Comparison of the shock-wave energy at a gage distance of 1.5 in. to the total initial electrical energy indicates that, on the average, 58 percent of the total initial electrical energy is converted to shock-wave energy. This figure is supported by independent investigators.

6. Because the usual techniques for determining the explosion time constant in chemical experiments cannot be utilized in this study, an approximation based upon certain assumptions is made such that:

$$\tau_e = 2t_{max} - \tau_a$$

where τ_e is the explosion time constant for the EWP event, τ_{max} is the total rise time measured from zero pressure to peak pressure, and τ_a is a characteristic time constant (the sum of the

amplifier rise time and the transit time of the explosion wave across the crystal). By calculation, τ_a is 3.41 μsec. The average of t_{max} for 43 shots is 3.42 μsec. Therefore, the calculations involving τ_e and τ_a are given some reason for confidence.

7. The principle of similarity (and the Kirkwood-Bethe theory consequently) predicts increasing time duration with propagation. The time measurements of the oscillographic records (θ_1, θ_2, θ_3, θ_4, θ_5, and t_{max}) show evidence of profile broadening for θ_5 and t_{max} only. The other time measurements should, but do not, show the same trend. In the case of θ_5 and t_{max}, the increase in duration is gentle but sufficiently evident to be recognized.

8. The time measurement (t_{max}) is altered to give the reduced time constant for EWP data and is plotted against its corresponding value of $W^{1/3}/R$, the scaled reciprocal distance. This comparison shows that the reduced time constant for EWP is of the same order of magnitude as CUE data, but that EWP values are larger. This comparison shows further that the reduced time constant does form a similarity curve as does CUE data. Finally, because of the negative slope, this comparison shows evidence of profile broadening; however slight, it is nonetheless distinguishable. The reduced time constant is given by the empirical formula:

$$(\tau_e/W^{1/3}) = 70\ (W^{1/3}/R)^{-0.22}$$

9. The data taken at $R = 1.5$ in. and some at $R = 3.0$ in. show a secondary peak pressure having a positive amplitude of 0.30 p_m of the first peak-pressure amplitude. A speculative guess as to the origin leads the author to believe that current dwell and subsequent reignition (a second, but lesser explosion) take place. Correlated electrical and optical measurements (not made in this study) would resolve this question.

10. Much of the data taken at $R \geq 7.5$ in. show a large negative pressure (a reflected shock wave) incident roughly 17 μsec after the peak pressure of the explosion wave. Since the tank dimensions preclude reflections from the sides and bottom of the tank, this reflection must be from the air-water interface. This conclusion is supported by calculation.

ACKNOWLEDGMENTS

The author wishes to express his gratitude to Dr. Macolm C. Henderson for his sustained encouragement during the course of this work and to Dr. M. F. M. Osborne, whose time, experience, and patience the author drew upon with countless interruptions. Further, the author wishes to acknowledge the very capable assistance of Mr. Paul I. Peterson and Mr. William J. Vaughan, both in the conduct of the experiment and for the useful discussions related to this study.

The nature of this study required consultations with many people, some outside NRL. The author wishes to acknowledge the informative conversations with Miss Ermine M. Christian about underwater explosions, Dr. Donna Price about chemical detonation processes, both of the Naval Ordnance Laboratory (Silver Spring, Md.) and Mr. John P. Slifko of the Naval Ordnance Laboratory Unit (Indian Head, Md.) for the material assistance rendered, in addition to the useful discussions.

The author is further indebted to Dr. F. D. Bennett of the Ballistics Research Laboratories (Aberdeen Proving Ground, Md.) for his helpful comments.

Finally, the author wishes to acknowledge the advice, support, and services rendered by NRL personnel, too numerous to list here, but gratefully remembered.

REFERENCES

1. Nairne, E., "Electrical Experiments," *Phil. Trans. Roy. Soc.* (London) **13**:498-502 (1774)
2. Chace, W. G., and Watson, E. M., "A Bibliography of Electrically Exploded Conductor Phenomena," AFCRC-TN-58-457, ASTIA Doc. No. AD-152640, Nov. 1958
3. McGrath, J. R., "Exploding Wire Research, 1774-1963," NRL Doc. 345605, June 1963
4. Chace, W. G., and Moore, H. K., editors, "Exploding Wires," Vols. I, II, and III, New York:Plenum Press, 1959-1965. (a) Moses, K. G., and Korneff, T., "The Nonlinear Effects of an Air Gap Switch in Exploding Wire Circuit," Vol. III, 1965; and (b) Buntzen, R. R., "The Use of Exploding Wires in the Study of Small Scale Underwater Explosions," Vol. II, 1962
5. Bennett, F. D., "Exploding Wires," *Sci. Am.* **206(5):**103-112 (May 1962)
6. Chace, W. G., *Phys. Today* **17(8):**19-24 (1964)
7. Hilliar, H. W., British Dept. of Scientific Research and Experiment Rept. RE 142/19 (1919)
8. Snay, H. G., "The Scaling of Underwater Explosion Phenomena," Naval Ordnance Lab. NOLTR 61-46, June 1961
9. Kennard, E. H., "Report on Underwater Explosions," David Taylor Model Basin Rept. 480, 1941
10. Underwater Explosion Research, "The Shock Wave," Vol. 1, Office of Naval Research, 1950
11. Cole, R. H., "Underwater Explosions," Princeton Univ. Press, 1948. (a) p. 182; and (b) pp. 143-144
12. Kirkwood, J. G., and Bethe, H. A., "The Pressure Wave Produced by an Underwater Explosion," OSRD 588, May 1942
13. Duhamel, J. E., Polytech., Paris 14, Cah 22, p. 20, 1833; also see Durand, W. F., editor, "Aerodynamic Theory," Vol. V, Sec. N, Berlin:Springer, 1935; also see Cheng, D. K., "Analysis of Linear Systems," Reading, Mass.:Addison-Wesley, p. 241, 1959
14. Osborne, M. F. M., *J. Appl. Phys.* **14:**180-184 (Apr. 1943)
15. Vaughan, W. J., "Underwater Shock Waves Formed by Exploding Wires," NRL Report 5901, Apr. 1963
16. Price, D., *Chem. Rev.* **59:**805 (1959)
17. Mehlart, L. J., "Magnetic Blow Out Switch," Patent 2,936,390, May 10, 1960
18. Page, L., "Introduction to Theoretical Physics," 3rd edition, New York:Van Nostrand, pp. 89-90, 1959
19. Arons, A. B., and Cole, R. H., *Rev. Sci. Instr.* **21:**30-38 (1950)
20. Fox, F. E., Herzfeld, K. F., and Rock, G. D., *Phys. Rev.* **70:**329-339 (1946)
21. Arons, A. B., and Yennie, D. B., "Long Range Shock Phenomena in Underwater Explosion Phenomena, I," NavOrd Rept. 424 (Unclassified), Apr. 1949
22. Bebb, A. H., *Phil. Trans. Roy. Soc.* (London) (Series A) **244:**153-175 (1951)
23. Coles, J. S., *et al.*, "Shock Wave Parameters from Spherical HBX and TNT Charges Detonated Underwater," WHOI Underwater Explosives Research Lab., NavOrd Rept. 103-46, Dec. 1946
24. Arons, A. B., *J. Acoust. Soc. Am.* **26(3):**343, 344 (1954)
25. "Underwater Nuclear Explosions," *Interavia* **17(11):**1428-1433 (1962)
26. Bennett, F. D., *Phys. Fluids* **5(1):**110 (1962); also Bennett, F. D., Burden, H. S., and Shear, D. D., "Correlated Electrical and Optical Measurements of Exploding Wires," p. 23, Aberdeen Proving Ground, Ballistic Research Laboratory Rept. 1133, June 1961
27. Osborne, M. F. M., and Taylor, A. H., *Phys. Rev.* **70:**322-328 (1946)
28. Gilstein, J. B., "Bubbles Produced by Submerged Exploding Wires," N.Y. Univ. Contract NR 062193, Dec. 1955

Security Classification

DOCUMENT CONTROL DATA - R&D

(Security classification of title, body of abstract and indexing annotation must be entered when the overall report is classified)

1. ORIGINATING ACTIVITY *(Corporate author)*	2a. REPORT SECURITY CLASSIFICATION
U.S. Naval Research Laboratory Washington, D.C., 20390	UNCLASSIFIED
	2b. GROUP

3. REPORT TITLE

Scaling Underwater Exploding Wires

4. DESCRIPTIVE NOTES *(Type of report and inclusive dates)*

An interim report on one phase of the problem.

5. AUTHOR(S) *(Last name, first name, initial)*

McGrath, James R.

6. REPORT DATE	7a. TOTAL NO. OF PAGES	7b. NO. OF REFS
December 17, 1965	30	28

8a. CONTRACT OR GRANT NO.	9a. ORIGINATOR'S REPORT NUMBER(S)
NRL Problem E01-01 b. PROJECT NO. ONR Problem RR 010-04-41-5950 c. BuShips SR 007-12-01-0800 d.	NRL Report 6266
	9b. OTHER REPORT NO(S) *(Any other numbers that may be assigned this report)*

10. AVAILABILITY/LIMITATION NOTICES

No restrictions

11. SUPPLEMENTARY NOTES	12. SPONSORING MILITARY ACTIVITY
	Department of the Navy (Bureau of Ships) (Office of Naval Research)

13. ABSTRACT

Five-mil Nichrome wires have been exploded under water using a 1/2-μf capacitor which stored energy up to 100 joules. The results indicate that peak pressure scales like a chemical explosive if losses due to the circuit and joule heating of the wire itself are accounted for. On this basis, the equivalent weight of TNT represented by the electrical energy stored in the capacitor is

$$W = 525(0.325CV_0^2 - E_V)/H_D$$

where W is the weight in micropounds, C is the capacitance in farads, V_0 is the initial charging voltage, E_V is the estimated energy dissipated by the wire in joules, and H_D is the heat of detonation of TNT in calories per gram. This scaling behavior extends the law of similarity six decades in terms of weight, from pounds to micropounds. The peak pressure for exploding-wire phenomena has been obtained from data and is empirically expressed as

$$p_m = 26{,}800\ (W^{1/3}/R)^{1.08}$$

where p_m is peak pressure and R is pressure-gage distance.

The instrument response to the short-duration shock wave gives rise to a new definition of the explosion constant τ_e. The reduced time-constant parameter shows qualitative agreement in value and slope with chemical data scales, and is given empirically as:

$$\frac{\tau_e}{W^{1/3}} = 70\left(\frac{W^{1/3}}{R}\right)^{-0.22}$$

DD FORM 1 JAN 64 1473

Security Classification

14. KEY WORDS	LINK A		LINK B		LINK C	
	ROLE	WT	ROLE	WT	ROLE	WT
Electrical explosion Capacitor discharge Similarity Underwater shock waves Underwater explosions Exploding wires						

INSTRUCTIONS

1. ORIGINATING ACTIVITY: Enter the name and address of the contractor, subcontractor, grantee, Department of Defense activity or other organization *(corporate author)* issuing the report.

2*a*. REPORT SECURITY CLASSIFICATION: Enter the overall security classification of the report. Indicate whether "Restricted Data" is included. Marking is to be in accordance with appropriate security regulations.

2*b*. GROUP: Automatic downgrading is specified in DoD Directive 5200.10 and Armed Forces Industrial Manual. Enter the group number. Also, when applicable, show that optional markings have been used for Group 3 and Group 4 as authorized.

3. REPORT TITLE: Enter the complete report title in all capital letters. Titles in all cases should be unclassified. If a meaningful title cannot be selected without classification, show title classification in all capitals in parenthesis immediately following the title.

4. DESCRIPTIVE NOTES: If appropriate, enter the type of report, e.g., interim, progress, summary, annual, or final. Give the inclusive dates when a specific reporting period is covered.

5. AUTHOR(S): Enter the name(s) of author(s) as shown on or in the report. Enter last name, first name, middle initial. If military, show rank and branch of service. The name of the principal author is an absolute minimum requirement.

6. REPORT DATE: Enter the date of the report as day, month, year; or month, year. If more than one date appears on the report, use date of publication.

7*a*. TOTAL NUMBER OF PAGES: The total page count should follow normal pagination procedures, i.e., enter the number of pages containing information.

7*b*. NUMBER OF REFERENCES: Enter the total number of references cited in the report.

8*a*. CONTRACT OR GRANT NUMBER: If appropriate, enter the applicable number of the contract or grant under which the report was written.

8*b*, 8*c*, & 8*d*. PROJECT NUMBER: Enter the appropriate military department identification, such as project number, subproject number, system numbers, task number, etc.

9*a*. ORIGINATOR'S REPORT NUMBER(S): Enter the official report number by which the document will be identified and controlled by the originating activity. This number must be unique to this report.

9*b*. OTHER REPORT NUMBER(S): If the report has been assigned any other report numbers *(either by the originator or by the sponsor)*, also enter this number(s).

10. AVAILABILITY/LIMITATION NOTICES: Enter any limitations on further dissemination of the report, other than those imposed by security classification, using standard statements such as:

(1) "Qualified requesters may obtain copies of this report from DDC."

(2) "Foreign announcement and dissemination of this report by DDC is not authorized."

(3) "U. S. Government agencies may obtain copies of this report directly from DDC. Other qualified DDC users shall request through

_____."

(4) "U. S. military agencies may obtain copies of this report directly from DDC. Other qualified users shall request through

_____."

(5) "All distribution of this report is controlled. Qualified DDC users shall request through

_____."

If the report has been furnished to the Office of Technical Services, Department of Commerce, for sale to the public, indicate this fact and enter the price, if known.

11. SUPPLEMENTARY NOTES: Use for additional explanatory notes.

12. SPONSORING MILITARY ACTIVITY: Enter the name of the departmental project office or laboratory sponsoring *(paying for)* the research and development. Include address.

13. ABSTRACT: Enter an abstract giving a brief and factual summary of the document indicative of the report, even though it may also appear elsewhere in the body of the technical report. If additional space is required, a continuation sheet shall be attached.

It is highly desirable that the abstract of classified reports be unclassified. Each paragraph of the abstract shall end with an indication of the military security classification of the information in the paragraph, represented as *(TS), (S), (C), or (U)*.

There is no limitation on the length of the abstract. However, the suggested length is from 150 to 225 words.

14. KEY WORDS: Key words are technically meaningful terms or short phrases that characterize a report and may be used as index entries for cataloging the report. Key words must be selected so that no security classification is required. Identifiers, such as equipment model designation, trade name, military project code name, geographic location, may be used as key words but will be followed by an indication of technical context. The assignment of links, roles, and weights is optional.